



HHS Public Access

Author manuscript

Wiley Interdiscip Rev Nanomed Nanobiotechnol. Author manuscript; available in PMC
2023 March 01.

Published in final edited form as:

Wiley Interdiscip Rev Nanomed Nanobiotechnol. 2022 March ; 14(2): e1756. doi:10.1002/wnan.1756.

Nanocarrier-Hydrogel Composite Delivery Systems for Precision Drug Release

Lauren E. Kass,

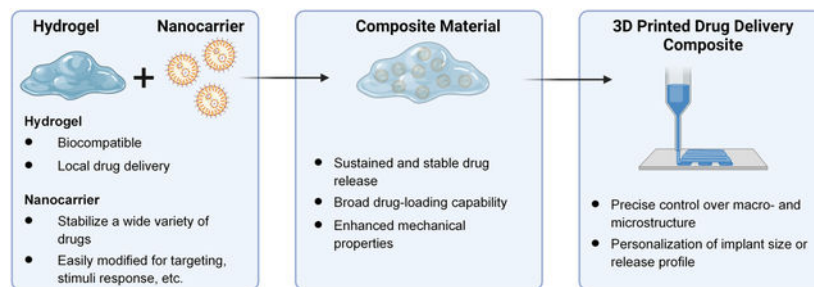
Juliane Nguyen *

Division of Pharmacoengineering and Molecular Pharmaceutics, Eshelman School of Pharmacy,
University of North Carolina at Chapel Hill, Chapel Hill, NC, 27599, USA

Abstract

Hydrogels are a class of biomaterials widely implemented in medical applications due to their biocompatibility and biodegradability. Despite the many successes of hydrogel-based delivery systems, there remain challenges to hydrogel drug delivery such as a burst release at the time of administration, a limited ability to encapsulate certain types of drugs (i.e., hydrophobic drugs, proteins, antibodies, and nucleic acids), and poor tunability of geometry and shape for controlled drug release. This review discusses two main important advances in hydrogel fabrication for precision drug release: first, the incorporation of nanocarriers to diversify their drug loading capability, and second, the design of hydrogels using 3D printing to precisely control drug dosing and release kinetics via high-resolution structures and geometries. We also outline ongoing challenges and discuss opportunities to further optimize drug release from hydrogels for personalized medicine.

Graphical Abstract



Nanocarrier-hydrogel composite materials can be engineered to improve drug delivery and may be implemented in 3D printing to create custom-designed drug delivery systems or tissue engineering implants.

Keywords

nanocarrier; hydrogel; 3D printing; personalized medicine

*Corresponding author: **Juliane Nguyen**, Division of Pharmacoengineering and Molecular Pharmaceutics, Eshelman School of Pharmacy, University of North Carolina at Chapel Hill, Chapel Hill, NC, 27599, USA, julianen@email.unc.edu.

1. INTRODUCTION

Hydrogels are a widely used class of biomaterials that are often implemented in medical applications because of their biocompatibility, biodegradability, and hydrophilicity (J. Li & Mooney, 2016). Hydrogels are attractive in drug delivery applications because of their ability to encapsulate hydrophilic drugs and provide sustained, locally targeted drug release, which can be tuned via the gel's physicochemical properties. Furthermore, hydrogel devices can be modified to provide sustained drug release to reduce administration frequency, which can lead to increased patient compliance.

Despite the successes of hydrogel-based delivery systems, challenges surrounding hydrogel drug delivery remain, such as (1) the presence of a burst release at the time of administration, (2) the limited ability to encapsulate certain categories of drugs (i.e. hydrophobic drugs, proteins, antibodies, and nucleic acids), and (3) the limited ability to fine-tune geometric patterns and shaped for precisely controlled drug release (Hoare & Kohane, 2008). This review discusses two main important strategies to customize and tailor hydrogels for precision and personalized therapeutics: first, the incorporation of nanocarriers to diversify the drug loading capability of hydrogels, and second, the design of hydrogels using 3D printing to precisely control drug dosing, release kinetics, and tailor it to the specific patient.

First, nanocarriers are a powerful tool to impart hydrogels with higher drug stability, enhanced mechanical properties, and the ability to encapsulate hydrophobic or easily denatured molecules. In addition, these carriers are attractive for drug delivery purposes as they have been shown to improve pharmacokinetics and drug distribution, and can provide targeted delivery via surface modifications (Din et al., 2017). Commonly used nanocarriers for drug delivery include liposomes, micelles, dendrimers, polymer-based particles, and nanotubes. Because of their synergistic effects when combined, nanocarriers have been incorporated into hydrogel drug delivery systems to enable both spatial and temporal control over drug release. These nanocarrier-hydrogel composite systems exhibit increased drug loading versatility. Furthermore, nanocarrier hydrogels can offer functional advantages, like increased mechanical reinforcement due to crosslinking between the carriers and hydrogel polymer chains (S. Yan et al., 2018), and dual-drug encapsulation in one delivery system (Zhu, Li, Liu, Chen, & Xi, 2012) (Figure 1). These composite scaffolds offer unique material properties and drug delivery capabilities, overcoming the challenges encountered using traditional nanocarrier or hydrogel systems alone.

Second, in the biomedical field, 3D printing (3DP) is emerging as a favorable method for generating personalized medical devices. Using 3DP, personalized hydrogel-based drug delivery devices can be designed with specific dosage amounts, combinations of drugs, and distinct release profiles based on the patient's unique physiology. This can be achieved through the design of complex, high-resolution geometries that are not available for hydrogel dosage forms produced in large-scale manufacturing processes. Moreover, 3DP is advantageous for the efficient and cost-effective generation of devices that can be easily modified simply by changing the composition of the material (Uziel, Shpigel, Goldin, & Lewitus, 2019). Common 3DP methods for drug delivery include extrusion printing, where

a material is deposited in a layer-by-layer fashion to form a 3D shape (i.e. fusion deposition modeling, syringe extrusion), and vat-polymerization printing, where a vat of liquid ink is crosslinked at very specific locations to build a solid structure (i.e. stereolithography, digital light processing) (Beg et al., 2020).

Overall, 3D printing can be used to customize nanocarrier-hydrogel composites for drug delivery, tissue engineering, and other disease applications (Chansoria et al., 2021). Hydrogels are easily implemented in 3D printing processes and can be formulated with specific properties for the intended application. Meanwhile, incorporation of nanocarriers into hydrogels can further expand the drug delivery capability of these 3D-printable devices. In this review, recent advancements in nanocarrier-hydrogel composite materials will be discussed with a specific emphasis on those systems which have been fabricated using 3DP, highlighting why these materials and this fabrication method compose a promising system for producing precision medical devices and therapeutics.

2. NANOCARRIER-HYDROGEL COMPOSITE MATERIALS OFFER UNIQUE ADVANTAGES FOR DRUG DELIVERY

2.1 LIPOSOMES MODULATE DRUG RELEASE KINETICS FROM HYDROGELS

Recently, the efficiency of liposomal drug delivery systems has been debated. Pharmacokinetic analysis shows that liposomes can accumulate in healthy tissues when administered intravenously, resulting in adverse side effects and compromising the therapeutic impact of the dose (Smits et al., 2019). Incorporating liposomes into hydrogels can enhance the mechanical properties of the liposome formulation and enable localized, sustained drug release, thereby improving ease of administration and delivery efficiency to the disease site (Mourtas et al., 2007). Liposomal hydrogels have been used to treat a variety of medical conditions, including spinal cord injury (X. Li et al., 2018), infection (Thapa, Kiick, & Sullivan, 2020), and cancer (Yin et al., 2020).

Liposomal hydrogels (Table 1) are advantageous for encapsulating both hydrophobic and hydrophilic molecules. For infection control in wounds, the hydrophilic antimicrobial Vancomycin was encapsulated in the aqueous core of the liposome (Thapa et al., 2020). Paclitaxel, which is hydrophobic, was delivered in liposomes via loading into the lipid bilayer (X. Li et al., 2018; Yin et al., 2020). This not only demonstrates the drug-loading versatility of liposomal delivery systems, but the ability to solubilize and stabilize hydrophobic drugs inside hydrogels. The hydrogel sustains liposome diffusion to the target site, after which the hydrophobic drug can diffuse from the liposome (Yin et al., 2020).

Drug release kinetics from hydrogels can be vastly optimized via liposome encapsulation. Thapa et al. showed that unencapsulated vancomycin inside collagen/fibrin co-gels for infection control can diffuse easily through the gel pores, resulting in a short period of release. When vancomycin was loaded into liposomes, drug release was prolonged 24 hours due to liposome retention inside the hydrogel and reduction of vancomycin mass transfer because of the lipid bilayer. When the liposomes were modified with collagen mimetic

peptide (CMP), release was prolonged by 36 hours due to increased liposome retention (Thapa et al., 2020).

Liposomes can be surface-modified for added functionality, as exemplified by the CMP-vancomycin liposomes developed by Thapa et al. CMPs can spontaneously fold into a triple helical structure and be incorporated into native collagen triple helices; thus, including CMPs on the liposome surface can aid in liposome retention inside collagen-based hydrogels (Thapa et al., 2020). Liu et al. developed antibacterial, adhesive liposomal hydrogels for bone reconstruction (L. Liu et al., 2019). Octadecylamine was linked to BMP-2-loaded liposomes to facilitate adhesive interactions to local tissues, thus improving BMP-2 retention at the reconstruction site.

Interestingly, liposomes can form supramolecular hydrogels via self-assembly, without the presence of a polymeric matrix. Pure liposomal hydrogels exhibit unique properties compared to liposome-in-hydrogel formulations. Pure liposomal hydrogels do not require the use of polymers and crosslinkers, minimizing the number of components in the system. Thus, these systems may pose fewer toxicity concerns, and face fewer barriers in regulatory approval processes. For example, Goergen et al. developed a hydrogel composed of self-assembled artificial single-chained bolalipids dotriacontane-1,1-diylbis [2-(trimethylamino)ethyl phosphate] (PC-C32-PC) and dotriacontane-1,1-diylbis [2-(dimethylamino)ethyl phosphate] (Me2PE-C32-Me2PE) (Goergen et al., 2019). It was found that the bolalipid hydrogels released a model drug 46% slower over 8 hours compared to a hydroxyethyl cellulose hydrogel, due to the hydrophobic interactions between the model drug and the bolalipid network. However, the mechanical strength of the hydrogel was significantly lower than that of polymeric hydrogels. Liu et al. developed liposomes modified with the block co-polymer poly(ethylene glycol)-polycaprolactone-poly(ethylene glycol) (PECE), which enables the liposomes to self-assemble in response to temperature (Meifeng Liu et al., 2020). During preparation the liposome solution is liquid, but upon cooling to room or physiological temperature, a hydrogel is formed. Hydrophilic drugs encapsulated within the liposome core exhibit slowed release due to the liposomal membrane, and because of the immobilization of the liposomes by PECE. Compared to a pure PECE hydrogel, drug release was reduced 38% after 12 hours when encapsulated in the pure liposome hydrogel. Similarly, Li et al. modified the surface of phosphatidylcholine liposomes with thiolated chitosan (R. Li et al., 2020). Thermosensitivity is imparted to the liposomes when beta-glycerophosphate solution is added, resulting in the formation of a hydrogel at physiological temperature, which is strengthened by disulfide bonds between adjacent liposomes. Drug release was tailored by modifying the liposome concentration; at higher concentrations, the release rate slowed, due to decreasing pore size. For the hydrogel containing the highest concentration of liposomes, drug release reached only 40% after 70 hours.

The physicochemical properties of the hydrogels can be tuned to provide additional control over drug release. Yin et al. developed a 3D scaffold based on waterborne polyurethane to encapsulate paclitaxel-loaded liposomes for the treatment of breast cancer (Yin et al., 2020). The scaffold degradation rate can be tuned via the gel porosity, which is related to the solid content of waterborne polyurethane during freeze-drying. Material degradation directly

impacts liposomal drug release, so the system imparts sustained yet tunable release profiles. Similarly, Mufamadi et al. developed a chitosan-based hydrogel loaded with liposomal galantamine for the treatment of Alzheimer's disease, and found that degradation, liposome size, and gel porosity influence drug release (Mufamadi et al., 2019). Gels with increased porosity, hydration rate, and swelling exhibited faster release kinetics. Additionally, larger liposomes (> 100 nm) diffused more slowly through the gel, slowing drug release.

Liposomal gels have been fabricated using polymers that confer useful properties for drug delivery. Qu et al. developed a thermosensitive liposomal hydrogel to deliver α -tocopherol for the treatment of myocardial infarction (Y. Qu et al., 2019). The hydrogel is composed of chitosan/ β -glycerol phosphate disodium salt, which undergoes a sol-to-gel phase transition at 33.8°C. This phase transition makes the gel an attractive candidate for an injectable formulation. The hydrogel developed by Liu et al. has the unique ability to self-heal (L. Liu et al., 2019). Disulfide bonds and crosslinks between sulfhydryl groups and silver ions which form the hydrogel may be broken under mechanical stress, but are formed again when contact is reinitiated, which is advantageous for injectable hydrogels which are constantly exposed to mechanical forces.

Liposomal hydrogels are particularly advantageous for gene delivery applications. While liposomes, which are commonly used to deliver nucleic acid cargoes, protect the therapeutic from degradation, hydrogels sustain liposome/gene release, and can be used to direct interactions with the surrounding microenvironment. Schwabe et al. developed a lipopolyplex-loaded gelatin hydrogel for the controlled release of siRNA (Schwabe et al., 2017). Lipopolyplex distribution in the gelatin hydrogels was found to be homogenous, and hydrogel formulation effectively controlled siRNA release. Hydrogels with lower crosslinking densities and a porous morphology showed faster rates of siRNA release. Moreover, anti-luciferase siRNA-loaded lipopolyplex hydrogels could be used to successfully silence luciferase activity in SKOV-3-Luc cells. Furst et al. developed a lipoplex-in-hydrogel system for the vaginal delivery of siRNA (Furst et al., 2016). Hydroxyethyl cellulose hydrogels were loaded with PEG-modified lipoplexes, and subsequently freeze-dried. Release of siRNA was controlled as the hydrogel was rehydrated in vaginal mucus and was dependent on hydrogel concentration and viscosity.

Liposomal hydrogels also offer advantages for immunotherapy options. Chen et al. developed GFP-mRNA lipoplexes using StemFect™ and Lipofectamine™ liposomes, which were subsequently loaded into poly(2-hydroxyethyl methacrylate) (pHEMA) scaffolds (R. Chen, Zhang, Yan, & Bryers, 2018). Scaffolds were implanted in C57BL/6J, and transfection efficiency of the GFP-mRNA was evaluated via fluorescence imaging. Compared to naked mRNA delivered from pHEMA scaffolds and subcutaneous injections of lipoplexes, lipoplex-loaded hydrogels demonstrated higher transfection efficiency, owing to local lipoplex retention by the scaffold. Yan et al. developed a similar platform for vaccine applications using lipoplex-loaded chitosan/alginate hydrogels (J. Yan, Chen, Zhang, & Bryers, 2019). StemFect™ liposomes were complexed with ovalbumin mRNA and loaded into a hydrogel composed of *N*-succinyl-chitosan and oxidized alginate. IFN- γ secretion indicated that the lipoplex-loaded hydrogel was most effective at eliciting a T cell response compared to the administration of ovalbumin or naked mRNA.

Several recently developed liposomal hydrogels have been applied *in vivo*. Qu et al. injected their thermosensitive chitosan hydrogels subcutaneously in mice, and studied the gel degradation, biocompatibility, and antioxidant activity (Y. Qu et al., 2019). It was found that after six weeks *in vivo*, the gel was 50% degraded. It was also found that the hydrogels only caused a mild inflammatory response, and overall supported cardiomyocyte survival. Most importantly, the liposomal gel was able to inhibit reactive oxygen species production for cardiomyocytes under an oxidative stress environment. Thapa et al. tested their hydrogels *in vivo* to examine their antibacterial activity after multiple infections (Thapa et al., 2020). They showed that hydrogels containing CMP tethered liposomes were able to confer antimicrobial effects even after two rounds of infection, which would enable reduced dosing frequency. Liu et al. tested the ability of their adhesive liposomal hydrogels to promote osteogenic differentiation in rats with bone defects (L. Liu et al., 2019). They showed that compared to gels with non-adhesive liposomes, adhesive liposomal gels were better at promoting bone fracture healing.

2.2 MICELLAR HYDROGELS HAVE VERSATILE PROPERTIES THAT CONTROL DRUG RELEASE

Micelles are a popularly utilized drug carrier for highly insoluble drug molecules. In addition to their solubilizing and stabilizing ability, micelles also offer advantages such as reduced opsonin adhesion, increased circulation time, and ability to deliver multiple drugs or drugs and imaging contrast agents simultaneously (S. Kim, Shi, Kim, Park, & Cheng, 2010). When incorporated or formed into hydrogels, micelles can provide interesting material properties, such as stimuli-responsivity and enhanced mechanical strength (Peka , 2015) (Table 2).

Like liposomes, polymeric micelles have the ability to form supramolecular hydrogels via non-covalent interactions, thus not requiring encapsulation within a polymer matrix. Compared to micelle-loaded hydrogels, supramolecular micelle hydrogels are formed without any interactions with or damage to drug molecules due to covalent crosslinking, and are able to achieve higher micelle loading, thus higher drug loading within the gel (Dong, Pang, Su, & Zhu, 2015). Poudel et al. developed a hydrogel based on PEG-b-PCL micelles, which undergoes reversible gelation via host-guest interactions with α -cyclodextrin (α -CD), for the sustained delivery of doxorubicin (Poudel, He, Huang, Xiao, & Yang, 2018). Because gelation, thus mechanical properties and drug release rate, can be controlled with the α -CD concentration, this system offers great potential as an injectable dosage form. Similarly, Zhang et al. developed an MPEG-PCL block polymer hydrogel via host-guest interactions with α -CD for ocular delivery of diclofenac (Z. Zhang et al., 2016). Gelation time was tuned via the α -CD concentration, MPEG-PCL concentration, and type of MPEG-PCL block polymer used. Because the gel undergoes a gel-sol transition in response to shear forces (i.e. from blinking), sustained ocular drug release can be achieved. Mandracchia et al. developed a UV-crosslinkable micellar hydrogel via methacrylation of a polymeric micelle composed of inulin and vitamin E for beclamethasone dipropionate delivery to the colon (Mandracchia et al., 2018). Liu et al. developed a self-assembling hydrogel with thermoresponsive alginate-g-PNIPAAm copolymer micelles for the sustained delivery of doxorubicin (Min Liu, Song, Wen, Zhu, & Li, 2017). At physiological temperature, the

solution undergoes a sol-gel transition and slowly releases doxorubicin-loaded micelles, significantly increasing cellular uptake and minimizing drug resistance.

There are also advantages for developing hydrogels that incorporate micelles within the polymer matrix. Yu et al. developed a micellar hydrogel with carboxymethyl chitosan (CMC) as the polymer phase and poloxamer 407 (F127) as the micelle phase via a glutaraldehyde crosslinking reaction (S. Yu et al., 2017). The crosslinking of micelles to CMC rendered the gel thermoresponsive and improved the gel strength compared to the physical mixture of F127 micelles and CMC. Meanwhile, the biological properties of CMC serves to improve the biocompatibility of the gel. Qu et al. developed a hydrogel composed of quaternized chitosan and benzaldehyde terminated Pluronic® F127 micelles to deliver curcumin for wound healing (J. Qu et al., 2018). Using a dynamic Schiff base bond between the chitosan and the micelles in addition to crosslinking among the copolymer micelles, the gels exhibited excellent mechanical strength and self-healing ability.

Many micellar hydrogels exhibit responses to various stimuli, thus enabling great control over drug delivery. As previously mentioned, several recently developed systems are thermoresponsive, which make them great candidates for injectable formulations (Min Liu et al., 2017; S. Yu et al., 2017). Polymeric micelles, such as F127 and PNIPAAm, undergo self-assembly with a temperature increase. With gelation temperatures near physiological, the formulation may be injected as a liquid and quickly turn into a solid at body temperature, thus creating a sustained release depot. Precise control over the injection site and gelation speed of the system is important for ensuring the depot remains at the site of injection, rather than migrating away from the injection site and polymerizing in an undesirable location, which could cause embolism that could lead to brain stroke, myocardial infarction, organ damage or pulmonary embolism (Asai et al., 2012; L. Yu & Ding, 2008). The hydrogel developed by Yu et al. is also pH responsive due to the presence of carboxyl groups, which change charge states in response to pH, thus greatly impacting swelling behavior (S. Yu et al., 2017). Higher swelling correlated with faster drug release, which occurred at physiological pH compared to more acidic environments. In contrast, the hydrogel developed by Qu et al. for the treatment of infection in wounds, which exhibit slight acidity, showed faster drug release in more acidic environments (J. Qu et al., 2018). Higher swelling of chitosan occurred at acidic pH, contributing to faster degradation behavior. Gao et al. developed a pH-sensitive hydrogel composed of F127 micelles crosslinked to a chitosan/oxidized dextran polymer (Gao et al., 2016). The hydrogel was prepared with Schiff base bonds which are broken by hydrolysis, thus degradation is accelerated in acidic environments. Additionally, this system exhibits redox-sensitivity due to the presence of disulfide bonds in the F127 shell (Gao et al., 2016). Both of these conditions are exhibited in the tumor microenvironment, thus the system can provide “smart” delivery of anticancer drugs specifically to cancerous tissues. Wen et al. developed a glucose-sensitive micellar hydrogel composed of Zwitterionic dialdehyde starch-based micelles for the treatment of diabetes (Wen et al., 2019). The micelles were crosslinked to a chitosan-based polymer via Schiff base bonds and loaded with insulin. When the identifying groups within the micelles recognize glucose, they turn hydrophilic, which causes the micelle structure to collapse and release the encapsulated insulin.

Micellar hydrogels are also attractive because they enable dual delivery of hydrophilic and hydrophobic drugs simultaneously, which can improve the therapeutic impact of the formulation. Gao et al. used their hydrogel to encapsulate hydrophobic curcumin within the micelle core and dispersed hydrophilic 5-fluoracil within the hydrogel phase, thus enabling a synergistic anti-cancer effect (Gao et al., 2016). Similarly, Wen et al. used their hydrogels to deliver insulin, which was encapsulated inside of the micelle core, as well as nattokinase, which was dispersed within the hydrogel phase (Wen et al., 2019). Nattokinase is a thrombolytic agent that is used to treat vascular diabetes complications. The combined drug delivery results in a synergistic therapeutic effect.

Several of the recently developed micellar hydrogels have been studied *in vivo*. The hydrogel developed by Qu et al. for wound healing was tested in a full-thickness skin defect model (J. Qu et al., 2018). The antibacterial quaternized chitosan in the gels provided an increased therapeutic effect compared to control groups, and when curcumin was encapsulated within the micelles, wound healing was even further accelerated. Zhang et al. tested their micellar hydrogel for ocular drug delivery in rabbit eyes (Z. Zhang et al., 2016). They showed that their micellar hydrogel did not cause any ocular irritation and increased ocular bioavailability of diclofenac compared to micellar formulations.

2.3 DENDRIMERS STABILIZE HYDROPHOBIC DRUGS IN HYDROGEL MATRICES FOR PROLONGED RELEASE

Dendrimers are branched polymeric structures that can carry hydrophobic or hydrophilic drug molecules via host-guest interactions or covalent bonding. Dendrimers can be optimized in their surface charge, size, and water solubility depending on the route of administration and the drug being delivered. Additionally, dendrimers can be actively targeted to disease sites via surface modifications with targeting moieties. However, the use of dendrimers as drug carriers may be limited because of their high cost of synthesis and potential toxicity (Madaan, Kumar, Poonia, Lather, & Pandita, 2014).

Polyamidoamine (PAMAM) dendrimers are particularly attractive for drug delivery because of their non-immunogenicity, water solubility, biodegradability, and biocompatibility. These dendrimers can be used to entrap molecules within the dendrimer void; alternatively, drug molecules can be covalently attached to the branched dendrimer chains. Recently, a new class of hydrogels have been developed by using PAMAM dendrimers to mildly crosslink polymer chains (Table 3). These hydrogels are therefore able to stabilize hydrophobic drugs within the hydrogel phase, which enables sustained and controlled drug release, mainly for the treatment of cancer (Abedi-Gaballu et al., 2018).

Previously, dendrimer hydrogels were developed using photoinitiated polymerization (J. Wang, Cooper, He, Li, & Yang, 2018). However, this method generates UV-induced free radicals that can cause toxicity to cells. Wang et al. developed a method for synthesizing dendrimer microgels via copper-free click chemistry and aza-Michael addition (aMA) with poly(ethylene glycol) diacrylate (PEGDA) (J. Wang et al., 2018). Using the aMA synthesis method, gelation time and degradation is easily controlled, and the gels exhibit high elasticity. These dendrimer microgels were loaded with the anticancer drug camptothecin, and drug release via pH-sensitive microgel degradation was specific for the

tumor microenvironment. Using the same chemistry, a dendrimer hydrogel encapsulating brimonidine tartrate was developed for the treatment of glaucoma (J. Wang, Williamson, Lancina Iii, & Yang, 2017). Brimonidine is present in three forms in the dendrimer hydrogel: free base, salt, and encapsulation. The free base and salt forms of brimonidine are mainly present in the hydrogel phase and diffuse out of the gel rapidly in a burst release, whereas brimonidine in the dendrimer core is released more slowly, resulting in a two-phase drug release.

Because of similar concerns with photoinitiated polymerization, Xu et al. developed a PEG-based PAMAM dendrimer hydrogel using copper-free click chemistry (L. Xu, Cooper, Wang, Yeudall, & Yang, 2017). Using the poly(ethylene glycol) bisazide (PEGBA) chain length and ratio of the concentrations of dendrimer and PEGBA, the chemical and physical properties of the gels were optimized to maintain fluidity. Because of this unique property, the system has potential as an injectable dosage form. Wang et al. also developed an injectable dendrimer hydrogel formulation via the aMA reaction with PEGDA to deliver the anticancer drug 5-fluoracil (J. Wang, He, Cooper, & Yang, 2017). By varying the degree of dendrimer acetylation, the gelling behavior of the hydrogels was optimized for injectability. With a lower degree of acetylation and higher dendrimer concentration, gelation time was much shorter. In another injectable PEGDA hydrogel containing PAMAM dendrimers, Wang et al. conjugated that anti-cancer drug camptothecin to the dendrimer surface, as opposed to physically embedding the drug within the dendrimer (J. Wang, He, Cooper, Gui, & Yang, 2019). Via a self-cleaving mechanism through the ammonolysis of ester bonds, camptothecin is released from the dendrimer surface and can diffuse through the hydrogel phase, resulting in sustained drug delivery.

Several of these systems have been investigated *in vivo*. The dendrimer microgels developed by Wang et al. were injected into mice, and toxicity was evaluated (J. Wang et al., 2018). Following injection, the behavior of the mice was normal, and the cytokine levels in the blood did not indicate that the microgels caused any acute toxicity. The injectable dendrimer hydrogel for the delivery of 5-fluoracil was tested in a head and neck cancer model via intratumoral injection (J. Wang, He, et al., 2017). Compared to drug/PBS controls, the dendrimer hydrogel formulation resulted in significant reduction in tumor volume without any adverse health effects to the mice. Xu et al. showed that their dendrimer hydrogel system for the delivery of 5-fluoracil was effective at improving survival of HN12 tumor-bearing mice by suppressing tumor growth over 2-fold compared to control formulations at the end of the study (L. Xu et al., 2017). The dendrimer hydrogel system developed by Wang et al. for the delivery of camptothecin was tested in a head and neck cancer model in mice (J. Wang et al., 2019). Tumor inhibition was achieved with conjugated (self-cleaving) and physically embedded camptothecin. However, tumor inhibition was found to be more effective when camptothecin was conjugated to the dendrimer surface after day 16 compared to when the drug was physically embedded in the dendrimer.

2.4 POLYMERIC CARRIER-LOADED HYDROGELS OFFER SUSTAINED RELEASE OF FRAGILE MACROMOLECULES

Polymeric nanoparticles have been extensively used in drug delivery applications because of their tunable properties, which enable enhanced permeation and targeted delivery specifically to the disease site. Polymeric drug carriers have been used to deliver a wide variety of drugs (i.e. proteins, nucleic acids, small molecules) to treat a broad range of medical conditions (i.e. bone defects, infection) (Bennet & Kim, 2014). Recently, 3D scaffolds (used mainly in tissue engineering) have been modified with polymeric nanocarriers to provide drug delivery functionality (Table 4). The 3D scaffold used for tissue repair can thus be loaded with bioactive molecules that further guide or promote cell growth (Modaresifar, Hadjizadeh, & Niknejad, 2017). Through the use of polymeric nanoparticles, these molecules are protected from harsh, degradative environments and can be delivered in a sustained manner.

The incorporation of nanoparticles into polymeric hydrogels can impart useful properties to the gel, such as increased swelling. Modaresifar et al. developed a gelatin methacryloyl (GelMA)/chitosan hydrogel with incorporated chitosan nanoparticles for the delivery of an angiogenic growth factor (bFGF) (Modaresifar et al., 2017). The incorporation of the chitosan nanoparticles prolonged drug release, which was controlled via the hydrogel crosslinking degree, and increased swelling of the hydrogel, which is more suitable for cell growth. It was also shown that the GelMA/chitosan gels with bFGF-loaded chitosan particles were more favorable for maintaining cell viability *in vitro*. Similarly, Azizian et al. developed a chitosan/gelatin scaffold containing chitosan nanoparticles for the delivery of bFGF and bovine serum albumin (BSA) (Azizian, Hadjizadeh, & Niknejad, 2018). It was found that nanoparticle incorporation into the scaffolds provided greater porosity, swelling, and wettability, which are all valuable properties for cell growth. Additionally, sustained growth factor release was achieved, and translated to increased fibroblast proliferation *in vitro*.

Nanoparticle incorporation into gel scaffolds can impact other gel properties, such as thermosensitivity. Li et al. developed a thermoresponsive chitosan hydrogel with chitosan nanoparticles to deliver bone morphogenetic protein-2 plasmid DNA (pDNA-BMP2) for alveolar bone repair (H. Li et al., 2017). It was found that gels containing chitosan nanoparticles exhibited a shorter sol-gel transition time when exposed to physiological temperature, which is preferable for clinical applications.

Polymeric nanoparticles have been incorporated into hydrogels for antibacterial purposes. Zhang et al. developed a bioadhesive antibacterial poly(ethylene glycol) dimethacrylate (PEGDMA)-based hydrogel containing poly(lactic-co-glycolic) acid (PLGA) nanoparticles for the delivery of the antimicrobial drug ciprofloxacin (Y. Zhang et al., 2016). Even when exposed to high shear stress, the gel maintained its adhesivity and viscoelasticity. Using the PLGA nanoparticles, sustained antibiotic release and higher antibiotic retention was achieved, contrasting with burst release behavior from a ciprofloxacin-loaded hydrogel.

Polymer nanocarrier composite hydrogels have shown great promise in *in vivo* studies. The hydrogel developed by Li et al. was studied in a rat cranial bone defect model and a

beagle dog periodontitis model. They showed that the gel containing pDNA-BMP2-loaded chitosan nanoparticles was successful at promoting osteogenesis in both rats and dogs without causing any adverse side effects (H. Li et al., 2017). Furthermore, after 8-weeks post-surgery, high levels of bone reformation and nearly complete hydrogel degradation was observed. In a study by Shahrezaee et al., metformin-loaded gelatin nanocarriers were incorporated into a poly(lactic acid) (PLA)/polycaprolactone (PCL) hydrogel for the treatment of bone defects (Shahrezaee et al., 2018). Results showed that sustained delivery of metformin exhibited high osteoinductivity *in vivo* compared to scaffolds that did not contain metformin. Naseri-Nosar et al. developed a cellulose acetate (CLA)/PLA scaffold containing citalopram-loaded gelatin nanocarriers for the treatment of nerve defects (Naseri-Nosar, Salehi, & Hojjati-Emami, 2017). The 3D scaffold was implanted as a nerve conduit in rats and its nerve regeneration ability was evaluated. Compared to the negative control and citalopram-free scaffolds, the citalopram-loaded gelatin nanocarrier scaffold was most successful at promoting sciatic nerve fiber growth, suggesting its applicability in neural tissue engineering.

2.5 NANOTUBES SIMULTANEOUSLY ENCAPSULATE DRUGS AND PROVIDE STABILITY TO THE HYDROGEL

Nanotubes, specifically halloysite nanotubes (HNTs), have been used as drug delivery carriers because they can be functionalized with a wide variety of drug molecules for delivery to disease sites with low toxicity and high mechanical strength. Compared to traditionally used carbon nanotubes (CNTs), HNTs are lower in cost and have a larger lumen diameter, which allows the encapsulation of larger molecules (Fizir et al., 2018). Recently, HNTs have been incorporated into hydrogel scaffolds for sustained drug release and to provide mechanical reinforcement to the gel (Table 5). Ji et al. developed a gelatin hydrogel reinforced with ibuprofen-loaded HNTs for the management of pain associated with infection after bone-grafting operations (Ji et al., 2017). Compared to the neat gelatin scaffold, HNT-loaded scaffolds were over 300% more mechanically robust with mechanical properties comparable to cancellous bone. Compared to HNT and gelatin scaffold delivery of ibuprofen, HNT-loaded gelatin scaffolds exhibited prolonged release profiles. Similarly, Thilan De Silva et al. fabricated alginate-based nanofibrous scaffolds containing cephalixin-loaded HNTs via electrospinning (Thilan De Silva et al., 2018). It was found that the elastic moduli of HNT-loaded scaffolds were 3-fold higher than empty scaffolds. Release of the antimicrobial cephalixin was extended when drug-loaded HNTs were encapsulated within the scaffold. For tissue engineering applications, this antibacterial-scaffold could eliminate any present infectious bacteria in the surgical site, and further prevent infection through the sustained delivery of cephalixin.

Hydrogels containing HNTs have also been used for dual drug encapsulation. Zhang et al. developed a poly(L-lactide) (PLLA) scaffold containing HNTs for the simultaneous delivery of a hydrophobic and hydrophilic drug (X. Zhang et al., 2015). Hydrophilic polymyxin B sulfate was encapsulated in the HNTs, and hydrophobic dexamethasone was encapsulated in the PLLA phase. The hydrogels were electrospun into fiber mats, and tunable, sustained release profiles were obtained by modifying the concentration of HNTs in the fibers.

Boron nitride nanotubes (BNNTs) are another alternative to carbon nanotubes which offer greater biological stability and compatibility (Ciofani, 2010). Pour Khalili et al. developed a PCL scaffold with doxorubicin-loaded BNNTs as a potential transdermal drug delivery system (Pour Khalili, Moradi, Kavehpour, & Islamzada, 2020). The scaffolds fabricated using an electrospinning-electrospraying method, exhibit pH and temperature sensitivity. It was found that at high pH and lower temperatures, the release rate of doxorubicin is slowed. The release of doxorubicin was more stable from BNNTs inside the PCL scaffolds compared to free BNNTs.

3. 3D PRINTED NANOCARRIER-HYDROGEL SYSTEMS

3DP has emerged as an attractive tool for generating customized medical devices and drug delivery systems (Ahmad, Gopinath, & Dutta, 2019). There exists a broad range of 3DP processes, machines, and materials that can be optimized to fit the specific design parameters of custom medical devices. Recently, 3DP has been used to generate unique geometries of composite hydrogel-nanocarrier materials for patient-specific drug delivery and tissue engineering applications (Table 6). 3D-printed geometries with various surface areas and crosslinking densities may exhibit unique drug release kinetics due to the diffusional pathways of the drug and the dissolution rate of the structure itself (Figure 2).

The most commonly used methods for printing hydrogel-based scaffolds are extrusion-based (i.e. syringe-based extrusion, fused deposition modeling) or light-based (i.e. digital light processing). Extrusion-based 3DP includes methods in which a material is pushed through a nozzle and deposited layer-by-layer onto a surface. Extrusion 3DP is heavily reliant on the mechanical properties of the material. First, the gelation properties of the material must enable a low viscosity during extrusion through the nozzle, so that extremely high pressures are not required to dispense the material. This is especially important in the case of syringe-based extrusion, where materials are deposited through syringes with needles of small diameters for increased resolution. As such, shear-thinning materials are most appropriate for use in syringe-based extrusion 3DP, so that the material exhibits lower viscosities as it experiences high shear in the needle. Furthermore, the viscosity of the material must be high enough after extrusion to produce a self-supporting gel (Kirchmajer, Gorkin, & In Het Panhuis, 2013). Fused deposition modeling, another extrusion-based 3DP method that is typically employed in basic desktop printers, achieves this time-dependent control over rheological properties by heating a thermoplastic polymer above its glass transition temperature before depositing the polymer through the printer nozzle (Gnanasekaran et al., 2017). Typical disadvantages associated with extrusion-based 3DP methods include time-consuming material optimization and low-resolution printing. Because the resolution of the printed structure is highly dependent on material properties, rheological additives (i.e. nanoclays, nanotubes) may be used to help improve the gelation behavior of the material and thus increase the resolution. Light-based 3DP, such as digital light processing (DLP), may be used for systems that are photosensitive. DLP relies on the focused projection of UV light into a vat of liquid photopolymerizable material. The material is UV cured onto a stage at specific points based on computer-aided design into a solid structure. After a solid layer is cured, the stage is risen out of the vat so that the next layer of the structure can be photopolymerized. With DLP, printing is rapid and high-resolution compared to traditional

extrusion-printing techniques. Some disadvantages of this method is that the material must be modified with photocrosslinkable functional groups, and some photoinitiators used for crosslinking can produce cytotoxic free radicals (S. H. Kim et al., 2018).

Both extrusion-based and light-based methods have been used for the 3D printing of nanocarrier-hydrogel composites. Furthermore, nanocarriers are loaded into 3D printed scaffolds in two ways: they may be adsorbed onto the surface of a 3D printed structure or printed inside the ink. In 2015, Song et al. developed a 3D printed composite alginate hydrogel containing cyclosporin A-loaded PLGA microspheres (Song, Jang, Choi, Shim, & Cho, 2015). The alginate/PLGA microsphere gel was printed using a lab-built extrusion printer in the interior of a 3D printed PCL/PLGA scaffold. This was done to help mechanically reinforce the resulting structure, which was able to withstand compressive forces up to 10s of MPa. Fahimipour et al. 3D printed a tricalcium phosphate (TCP)-based hydrogel containing vascular endothelial growth factor (VEGF)-loaded PLGA microspheres (Fahimipour et al., 2017). The scaffold was printed via extrusion printing with the microspheres encapsulated in the composite ink. Using DLP, Xu et al. developed a GelMA hydrogel scaffold with monomethoxy poly(ethylene glycol)-poly(-caprolactone) (MPEG-PCL) micelles encapsulating RGFP966 for nerve regeneration (X. Xu et al., 2019). The micelles were mixed into a liquid GelMA resin, which was photopolymerized into a solid structure. Liu et al. developed a 3D printed a liposomal GelMA hydrogel patch loaded with doxorubicin (J. Liu, Tagami, & Ozeki, 2020). Using extrusion printing, drug-loaded liposomes were mixed into the GelMA-based ink to generate structures of three different geometries. Weisman et al. used a PLA hydrogel ink containing gentamicin-loaded HNTs for extrusion printing (Weisman, Jammalamadaka, Tappa, & Mills, 2017). The nanotubes act simultaneously as drug-releasing nanocontainers as well as a nanofiller for improving mechanical strength of the printed constructs.

Uniquely, Berry et al. (Berry, Díaz, Durand-Silva, & Smaldone, 2019) and Cho et al. (Cho et al., 2019) developed 3D printed micellar hydrogel scaffolds without the use of a polymeric network. Berry et al. printed F127-based hydrogels using extrusion printing. Viscous gel formulations were prepared by mixing F127 with a multi-arm thiol crosslinker. Viscous gels were 3D printed, then placed in a curing solution (basic PBS) for crosslinking via a thiol-Michael reaction, resulting in stabilized, mechanically robust 3D structures. Cho et al. took advantage of the sol-gel transition of poloxamer 407 micelles. An extrusion printing method was used to extrude the micelle solution at low temperature onto a heated plate, where the solution forms a gel. Micelles containing paclitaxel and rapamycin were printed into 3D disc structures.

An alternative method for generating 3D printed nanocarrier-hydrogels is to print the hydrogel phase of the scaffold, then subsequently adsorb the nanocarrier molecules to the scaffold surface using various reaction schemes. Wang et al. fabricated an extrusion-printed hydroxyapatite scaffold, which was then coated with crosslinked collagen via an EDC/NHS reaction (H. Wang et al., 2016). Chitosan microspheres containing rhBMP2 were then loaded onto the scaffold via a post-seeding technique. Sarkar et al. developed a 3D printed TCP scaffold, onto which curcumin-loaded liposomes were attached via thin-film hydration (Sarkar & Bose, 2019). Li et al. developed extrusion-printed PCL scaffolds that were

grafted with aspirin-loaded liposomes via an amine-catechol reaction onto a polydopamine coating (Y. Li et al., 2019, 2020). Similarly, Zhou et al. used a PDA coating to adsorb drug-loaded PLGA microspheres onto the surface of a PCL scaffold (Zhou et al., 2018). Zhang et al. developed a PLGA microsphere composite scaffold via microsphere adsorption onto a collagen-coated PCL scaffold (Z. Z. Zhang, Zhang, & Zhang, 2019). A 3D printed PCL-based scaffold for the treatment of bone defects developed by Ye et al. was loaded with liposomal nanocarriers via immersion in a ruthenium-loaded liposome suspension after printing (Ye et al., 2019). Even in these systems where post-processing steps are required to add nanocarriers to the implant, 3D printing is very useful for generating customizable shapes and hierarchical pore structures for controlling drug release. Thus, these scaffolds are especially attractive for drug delivery in tissue engineering applications.

As previously mentioned, the material properties of extrusion-printed structures must be considered and modified to optimize the printing resolution and mechanical properties of the resulting geometry. Fahimipour et al. incorporated gelatin into their TCP-based bioink to enable a thermoresponsive sol-gel transition (Fahimipour et al., 2017). It was found that the gel point increased with increasing content of gelatin. At 3% gelatin, the gel temperature of the solution was near room temperature, suggesting that the ink will extrude through the needle without clogging, but will also be able to maintain structural integrity after deposition. Ye et al. evaluated the rheological properties of their PCL-based scaffolds for shear-thinning behavior, which was exhibited by both of their ink formulations, suggesting both formulations are printable (Ye et al., 2019). Liu et al. used carboxymethyl cellulose (CMC) to increase the viscosity of their GelMA-based bioink (J. Liu et al., 2020). The formulations containing CMC exhibited shear-thinning properties, and the viscosity of the formulations increased in a CMC-dependent manner.

An advantage of 3D-printed drug delivery systems is that they may be customized to provide varying drug release profiles via different geometries and degrees of crosslinking. Liu et al. showed that both hydrogel geometry and degree of UV crosslinking may be used to tailor the drug release profile (J. Liu et al., 2020). They showed that while torus-shaped 3D-printed patches dissolve more quickly, thus resulting in a fast drug release, gridline and cylindrical patches dissolve more slowly, thus prolonging drug release. They noted that since cylindrical patches were not completely UV crosslinked, irregular release kinetics were observed. It was also observed in gridline patches that with longer UV exposure times, drug release was further sustained. Cho et al. showed that 3D-printed micellar hydrogel discs eliminated burst drug release compared to non-printed sol-gels, likely because of the quick erosion of sol-gels in physiological conditions (Cho et al., 2019). They further noted that while sol-gels must be kept at low temperatures before they are applied *in vivo*, discs may be maintained at room temperature until implantation, overall increasing the convenience of clinical handling.

Many of the previously mentioned 3D-printed composite hydrogels were applied *in vivo* to evaluate their toxicity and efficacy. These composite scaffolds are particularly useful for drug delivery in tissue repair applications, such as bone defect repair or nerve regeneration. Li et al. applied their 3D-printed PCL scaffolds containing bone forming peptide 1 and liposomal aspirin in a cranial defect animal model (Y. Li et al., 2020). Compared to scaffolds containing only one of the therapeutic molecules, the dual drug-loaded composite scaffold

exhibited the highest osteoinductive capacity. Zhang et al. tested their 3D-printed PCL/PLGA microsphere composite material *in vivo* to treat femur defects in rats (Z. Z. Zhang et al., 2019). It was found that the composite material resulted in complete defect healing after 12 weeks post-surgery, which is a vast improvement compared to the PCL scaffold alone. Xu et al. used 3D-printed GelMA-based nerve conduits to heal sciatic nerve defects in rats (X. Xu et al., 2019). They showed that the scaffolds were able to fully reconnect the distal and proximal sites of a 10 mm defect without complete degradation or collapse. Moreover, drug-loaded scaffolds exhibited faster nerve conducting velocity compared to empty scaffolds, demonstrating the impact of the sustained release of RGFP966.

3D-printed composite scaffolds have also shown great promise in non-tissue repair applications. Song et al. used 3D-printed alginate scaffolds containing drug-loaded PLGA microspheres for the management of immune responses associated with cell-based therapy (Song et al., 2015). The scaffolds were loaded with human lung fibroblasts and implanted subcutaneously in BALB/c mice. It was found that the sustained release of the immunosuppressive drug cyclosporin A enabled decreased mononuclear cell infiltration and decreased T-cell mediated rejection response. Furthermore, the integrity of the 3D-printed structures was maintained over a 4-week period *in vivo*. Cho et al.'s 3D-printed disc-shaped micellar scaffolds and non-printed micellar sol-gels loaded with paclitaxel and rapamycin were tested in ES-2-luc human ovarian-cancer-bearing xenograft mice (Cho et al., 2019). Though mice treated with discs showed a more substantial decrease in tumor volume than mice treated with sol-gels, their survival was nearly 1 week shorter than the sol-gel treated mice. It was determined that the decrease in median survival was due to mice that exhibited liver problems from reduced hepatic clearance of paclitaxel with the sustained-release disc scaffold. The authors note that in a future study, the dosing amount in the disc scaffolds will be optimized to reduce toxicity, since the surgical handling and therapeutic effect of the disc delivery systems were promising.

Conclusions and Perspectives

Nanocarrier-hydrogel composite drug delivery systems have attracted significant attention for controlled drug delivery and precision medicine. The incorporation of nanocarriers has significantly increased their drug loading versatility and potential therapeutic applications. Furthermore, recent advances in 3DP have been applied to print patient-specific hydrogel geometries to tailor drug release kinetics or serve as patient-specific tissue repair implants. A prevailing challenge in using this platform is ensuring drug and nanocarrier stability throughout the 3D printing process. These processes may expose the material and its contents to high temperatures, shear stress, or UV light, all of which have the potential to degrade encapsulated nanocarriers or drugs (Palo, Holländer, Suominen, Yliruusi, & Sandler, 2017).

While 3D-printed nanocarrier-hydrogel composites are showing great potential, these systems could benefit from additional optimization. Many of the geometries printed using these composite materials are of low resolution and are architecturally inadequate for precisely controlling drug release. Geometries that result in unique and more precise drug release kinetics are likely to require the use of light-based 3DP, as these devices

require high resolution that cannot be achieved with extrusion printing. As an example, microneedles are an advantageous architecture in drug delivery implants to improve drug penetration into target tissues. Using extrusion 3DP methods, it is very difficult to achieve micron-scale structures, as printing resolution depends heavily on the rheological properties of the material and the size of the needle from which the material is printed. Light-based 3DP can reach this level of precision and control; however, light-based 3DP methods are limited in the types of materials that can be printed and may compromise encapsulated drug or nanocarrier stability. Further exploration into the types of composite materials that are compatible with light-based 3DP to develop more complex architectures is warranted.

Nanocomposite materials will also be exposed to somewhat harsh conditions during 3D printing, such as shear stress and high temperature. As such, it is of vast importance to ensure nanocarrier and drug stability post-printing. Shear stress could potentially cause nanocarrier destabilization and degradation (Buxton, 2008), high temperatures may cause particle aggregation or increases in particle size, (B. Jonson, B. Lindmann, K. Holmberg, 1998). Encapsulated drugs also may undergo thermal or photo-degradation during printing (Trenfield, Awad, Goyanes, Gaisford, & Basit, 2018), though it is possible that the nanocarriers may offer protection from such damage (Hao et al., 2020; Woranuch & Yoksan, 2013). Nevertheless, drug release, degradation kinetics, and biocompatibility may be altered by the 3D printing process. Therefore, ensuring that the 3D printing process can generate devices consistently without compromising function or safety will be essential to clinical implementation.

There are extensive possibilities for the use of this class of 3D printed biomaterials. Furthermore, 4D printing is a technique in which a 3D printed structure can change shape in response to stimuli. This is particularly useful for surgical implantation of medical devices; the device may exhibit a compressed form during implantation through a small surgical site, then undergo expansion in the physiological environment (Wischke & Lendlein, 2010). Shape memory polymers used for 4D printing could potentially be combined with nanocarriers to preserve the drug delivery functionality of nanocarrier-hydrogel composite materials, but with improved surgical handling. Similarly, 3D printing *in vivo* has also recently gained some traction. 3D printing a structure *in situ* has the advantage of minimized exposure of the surgical site compared to implantation of a traditional 3D medical device. A proof of concept study showed the generation of a scaffold via *ex vivo* stimuli to control polymerization of a subcutaneously injected bioink (Y. Chen et al., 2020). It is possible that nanocarrier-hydrogel scaffolds could be formulated to be compatible with similar processes.

Though the nanocarrier-hydrogel composites described in this review involve a finite dose of drug encapsulated in the device, these materials may also be used to encapsulate cells that produce therapeutic biologics. This would allow for continuous drug production with cell persistence maintained via the hydrogel scaffold (Aliperta et al., 2017). Nanocarriers could be incorporated into the scaffold to provide dual drug delivery or to deliver essential nutrients or growth factors to the cells. However, ensuring that cell viability is preserved during the 3D printing process may be challenging, as cells may also be susceptible to high shear stress or UV light.

While nanocarrier-hydrogel composites can be advantageous for drug delivery purposes, the addition of nanoparticles makes them a complex material. To translate these materials to the clinic, robust characterization methods for the composites must be developed to ensure consistent physicochemical properties, mechanical properties, nanocarrier loading, and drug release. Moreover, the manufacturing and supply processes for these personalized materials may be complex and vastly different from conventional therapeutic devices, as the devices can be fabricated to be patient-specific. Thus, the design, preparation, characterization, transportation, and storage of the composite materials must be considered and streamlined to provide prompt, cost-effective, and tailored treatment for the patient.

Overall, 3D printed nanocarrier-hydrogel materials have the potential for use in a broad array of biomedical applications and with a wide variety of encapsulated payloads. Most importantly, their easy customizability makes them attractive materials for personalized medicine.

Acknowledgments

Figures created with [Biorender.com](https://biorender.com).

Funding Information

We acknowledge funding through the National Institutes of Health (R01CA241679 and R21GM135853).

References

- Abedi-Gaballu F, Dehghan G, Ghaffari M, Yekta R, Abbaspour-Ravasjani S, Baradaran B, ... Hamblin MR (2018). PAMAM dendrimers as efficient drug and gene delivery nanosystems for cancer therapy. *Applied Materials Today*, 12, 177–190. 10.1016/j.apmt.2018.05.002 [PubMed: 30511014]
- Ahmad N, Gopinath P, & Dutta R (2019). 3D printing technology in nanomedicine. *3D Printing Technology in Nanomedicine*. Elsevier. 10.1016/C2017-0-03828-4
- Aliperta R, Welzel PB, Bergmann R, Freudenberg U, Berndt N, Feldmann A, ... Bachmann MP (2017). Cryogel-supported stem cell factory for customized sustained release of bispecific antibodies for cancer immunotherapy. *Scientific Reports*, 7(1), 42855. 10.1038/srep42855
- Asai D, Xu D, Liu W, Garcia Quiroz F, Callahan DJ, Zalutsky MR, ... Chilkoti A (2012). Protein polymer hydrogels by in situ, rapid and reversible self-gelation. *Biomaterials*, 33(21), 5451–5458. 10.1016/j.biomaterials.2012.03.083 [PubMed: 22538198]
- Azizian S, Hadjizadeh A, & Niknejad H (2018). Chitosan-gelatin porous scaffold incorporated with Chitosan nanoparticles for growth factor delivery in tissue engineering. *Carbohydrate Polymers*, 202, 315–322. 10.1016/j.carbpol.2018.07.023 [PubMed: 30287006]
- Jonson B, Lindmann B, Holmberg K, K. B (1998). *Surfactant and polymers in aqueous solutions*, (Eds.), John Wiley and Sons, New York. Wiley.
- Beg S, Almalki WH, Malik A, Farhan M, Aatif M, Rahman Z, ... Rahman M (2020). 3D printing for drug delivery and biomedical applications. *Drug Discovery Today*. 10.1016/j.drudis.2020.07.007
- Bennet D, & Kim S (2014). Polymer Nanoparticles for Smart Drug Delivery. In *Application of Nanotechnology in Drug Delivery*. InTech. 10.5772/58422
- Berry DR, Díaz BK, Durand-Silva A, & Smaldone RA (2019). Radical free crosslinking of direct-write 3D printed hydrogels through a base catalyzed thiol-Michael reaction †. *Polymer Chemistry*, 10. 10.1039/c9py00953a
- Buxton GA (2008). The fate of a polymer nanoparticle subject to flow-induced shear stresses. *EPL (Europhysics Letters)*, 84(2), 26006. 10.1209/0295-5075/84/26006
- Chansoria P, Etter E, & Nguyen J (2021). Regenerating dynamic organs using biomimetic patches. *Trends in Biotechnology*. 10.1016/j.tibtech.2021.07.001

- Chen R, Zhang H, Yan J, & Bryers JD (2018). Scaffold-mediated delivery for non-viral mRNA vaccines. *Gene Therapy*, 25(8), 556–567. 10.1038/s41434-018-0040-9 [PubMed: 30242259]
- Chen Y, Zhang J, Liu X, Wang S, Tao J, Huang Y, ... Gou M (2020). Noninvasive in vivo 3D bioprinting. *Science Advances*, 6(23), eaba7406. 10.1126/sciadv.aba7406
- Cho H, Jammalamadaka U, Tappa K, Egbulefu C, Prior J, Tang R, & Achilefu S (2019). 3D Printing of Poloxamer 407 Nanogel Discs and Their Applications in Adjuvant Ovarian Cancer Therapy. 10.1021/acs.molpharmaceut.8b00836
- Ciofani G (2010, August). Potential applications of boron nitride nanotubes as drug delivery systems. *Expert Opinion on Drug Delivery*. Taylor & Francis. 10.1517/17425247.2010.499897
- Din FU, Aman W, Ullah I, Qureshi OS, Mustapha O, Shafique S, & Zeb A (2017). Effective use of nanocarriers as drug delivery systems for the treatment of selected tumors. *International Journal of Nanomedicine*, Volume 12, 7291–7309. 10.2147/IJN.S146315 [PubMed: 29042776]
- Dong R, Pang Y, Su Y, & Zhu X (2015). Supramolecular hydrogels: synthesis, properties and their biomedical applications. *Biomaterials Science*, 3(7), 937–954. 10.1039/c4bm00448e [PubMed: 26221932]
- Fahimipour F, Rasoulianboroujeni M, Dashtimoghadam E, Khoshroo K, Tahriri M, Bastami F, ... Tayebi L (2017). 3D printed TCP-based scaffold incorporating VEGF-loaded PLGA microspheres for craniofacial tissue engineering. *Dental Materials*, 33(11), 1205–1216. 10.1016/j.dental.2017.06.016 [PubMed: 28882369]
- Fizir M, Dramou P, Dahiru NS, Ruya W, Huang T, & He H (2018, August 1). Halloysite nanotubes in analytical sciences and in drug delivery: A review. *Microchimica Acta*. Springer-Verlag Wien. 10.1007/s00604-018-2908-1
- Furst T, Dakwar GR, Zagato E, Lechanteur A, Remaut K, Evrard B, ... Piel G (2016). Freeze-dried mucoadhesive polymeric system containing pegylated lipoplexes: Towards a vaginal sustained released system for siRNA. *Journal of Controlled Release*, 236, 68–78. 10.1016/j.jconrel.2016.06.028 [PubMed: 27329774]
- Gao N, Lü S, Gao C, Wang X, Xu X, Bai X, ... Liu M (2016). Injectable shell-crosslinked F127 micelle/hydrogel composites with pH and redox sensitivity for combined release of anticancer drugs. *Chemical Engineering Journal*, 287, 20–29. 10.1016/j.cej.2015.11.015
- Gnanasekaran K, Heijmans T, van Bennekom S, Woldhuis H, Wijnia S, de With G, & Friedrich H (2017). 3D printing of CNT- and graphene-based conductive polymer nanocomposites by fused deposition modeling. *Applied Materials Today*, 9, 21–28. 10.1016/j.apmt.2017.04.003
- Goergen N, Wojcik M, Drescher S, Pinnapireddy SR, Brüßler J, Bakowsky U, & Jedelská J (2019). The Use of Artificial Gel Forming Bolalipids as Novel Formulations in Antimicrobial and Antifungal Therapy. *Pharmaceutics*, 11(7), 307. 10.3390/pharmaceutics11070307 [PubMed: 31266209]
- Hao L, Gong L, Chen L, Guan M, Zhou H, Qiu S, ... Akbulut M (2020). Composite pesticide nanocarriers involving functionalized boron nitride nanoplatelets for pH-responsive release and enhanced UV stability. *Chemical Engineering Journal*, 396, 125233. 10.1016/j.cej.2020.125233
- Hoare TR, & Kohane DS (2008). Hydrogels in drug delivery: Progress and challenges. *Polymer*, 49(8), 1993–2007. 10.1016/j.polymer.2008.01.027
- Ji L, Qiao W, Zhang Y, Wu H, Miao S, Cheng Z, ... Zhu A (2017). A gelatin composite scaffold strengthened by drug-loaded halloysite nanotubes. *Materials Science and Engineering: C*, 78, 362–369. 10.1016/j.msec.2017.04.070
- Kim SH, Yeon YK, Lee JM, Chao JR, Lee YJ, Seo YB, ... Park CH (2018). Precisely printable and biocompatible silk fibroin bioink for digital light processing 3D printing. *Nature Communications*, 9(1), 1620. 10.1038/s41467-018-03759-y
- Kim S, Shi Y, Kim JY, Park K, & Cheng J-X (2010). Overcoming the barriers in micellar drug delivery: loading efficiency, in vivo stability, and micelle–cell interaction. *Expert Opinion on Drug Delivery*, 7(1), 49–62. 10.1517/17425240903380446 [PubMed: 20017660]
- Kirchmajer DM, Gorkin R, & In Het Panhuis M (2013). An overview of the suitability of hydrogel-forming polymers for extrusion-based 3D-printing. *J. Name*, 00, 1–3. 10.1039/x0xx00000x
- Li H, Ji Q, Chen X, Sun Y, Xu Q, Deng P, ... Yang J (2017). Accelerated bony defect healing based on chitosan thermosensitive hydrogel scaffolds embedded with chitosan nanoparticles for the delivery

- of BMP2 plasmid DNA. *Journal of Biomedical Materials Research Part A*, 105(1), 265–273. 10.1002/jbm.a.35900 [PubMed: 27636714]
- Li J, & Mooney DJ (2016). Designing hydrogels for controlled drug delivery. *Nature Reviews Materials*, 1(12), 16071. 10.1038/natrevmats.2016.71
- Li R, Lin Z, Zhang Q, Zhang Y, Liu Y, Lyu Y, ... Li L (2020). Injectable and In Situ -Formable Thiolated Chitosan-Coated Liposomal Hydrogels as Curcumin Carriers for Prevention of In Vivo Breast Cancer Recurrence. *ACS Applied Materials & Interfaces*, 12(15), 17936–17948. 10.1021/acsami.9b21528 [PubMed: 32208630]
- Li X, Fan C, Xiao Z, Zhao Y, Zhang H, Sun J, ... Dai J (2018). A collagen microchannel scaffold carrying paclitaxel-liposomes induces neuronal differentiation of neural stem cells through Wnt/ β -catenin signaling for spinal cord injury repair. 10.1016/j.biomaterials.2018.08.037
- Li Y, Bai Y, Pan J, Wang H, Li H, Xu X, ... Wei S (2019). A hybrid 3D-printed aspirin-laden liposome composite scaffold for bone tissue engineering †. *J. Mater. Chem. B*, 7, 619. 10.1039/c8tb02756k [PubMed: 32254795]
- Li Y, Li Q, Li H, Xu X, Fu X, Pan J, ... Wei S (2020). An effective dual-factor modified 3D-printed PCL scaffold for bone defect repair. *Journal of Biomedical Materials Research Part B: Applied Biomaterials*, 108(5), 2167–2179. 10.1002/jbm.b.34555 [PubMed: 31904173]
- Liu J, Tagami T, & Ozeki T (2020). Fabrication of 3D-printed fish-gelatin-based polymer hydrogel patches for local delivery of pegylated liposomal doxorubicin. *Marine Drugs*, 18(6). 10.3390/md18060325
- Liu L, Xiang Y, Wang Z, Yang X, Yu X, Lu Y, ... Cui W (2019). Adhesive liposomes loaded onto an injectable, self-healing and antibacterial hydrogel for promoting bone reconstruction. *NPG Asia Materials*, 11(1), 81. 10.1038/s41427-019-0185-z
- Liu Meifeng, Chen W, Zhang X, Su P, Yue F, Zeng S, & Du S (2020). Improved surface adhesion and wound healing effect of madecassoside liposomes modified by temperature-responsive PEG-PCL-PEG copolymers. *European Journal of Pharmaceutical Sciences*, 151, 105373. 10.1016/j.ejps.2020.105373
- Liu Min, Song X, Wen Y, Zhu JL, & Li J (2017). Injectable Thermoresponsive Hydrogel Formed by Alginate-g-Poly(N-isopropylacrylamide) That Releases Doxorubicin-Encapsulated Micelles as a Smart Drug Delivery System. *ACS Applied Materials and Interfaces*, 9(41), 35673–35682. 10.1021/acsami.7b12849 [PubMed: 28937214]
- Madaan K, Kumar S, Poonia N, Lather V, & Pandita D (2014). Dendrimers in drug delivery and targeting: Drug-dendrimer interactions and toxicity issues. *Journal of Pharmacy and Bioallied Sciences*, 6(3), 139–150. 10.4103/0975-7406.130965 [PubMed: 25035633]
- Mandracchia D, Trapani A, Perteghella S, Di Franco C, Torre M, Calleri E, & Tripodo G (2018). A Micellar-Hydrogel Nanogrid from a UV Crosslinked Inulin Derivative for the Simultaneous Delivery of Hydrophobic and Hydrophilic Drugs. *Pharmaceutics*, 10(3), 97. 10.3390/pharmaceutics10030097 [PubMed: 30029476]
- Manoukian OS, Arul MR, Rudraiah S, Kalajzic I, & Kumbar SG (2019). Aligned microchannel polymer-nanotube composites for peripheral nerve regeneration: Small molecule drug delivery. *Journal of Controlled Release*, 296, 54–67. 10.1016/j.jconrel.2019.01.013 [PubMed: 30658124]
- Modaresifar K, Hadjizadeh A, & Niknejad H (2017). Design and fabrication of GelMA/chitosan nanoparticles composite hydrogel for angiogenic growth factor delivery. *Artificial Cells, Nanomedicine, and Biotechnology*, 46(8), 1–10. 10.1080/21691401.2017.1392970
- Mourtas S, Fotopoulou S, Duraj S, Sfika V, Tsakiroglou C, & Antimisiaris SG (2007). Liposomal drugs dispersed in hydrogels. Effect of liposome, drug and gel properties on drug release kinetics. *Colloids and Surfaces B: Biointerfaces*, 55(2), 212–221. 10.1016/j.colsurfb.2006.12.005 [PubMed: 17223020]
- Mufamadi MS, Kumar P, du Toit LC, Choonara YE, Obulapuram PK, Modi G, ... Pillay V (2019). Liposome-embedded, polymeric scaffold for extended delivery of galantamine. *Journal of Drug Delivery Science and Technology*, 50, 255–265. 10.1016/j.jddst.2019.02.001
- Naseri-Nosar M, Salehi M, & Hojjati-Emami S (2017). Cellulose acetate/poly lactic acid coaxial wet-electrospun scaffold containing citalopram-loaded gelatin nanocarriers for neural tissue

- engineering applications. *International Journal of Biological Macromolecules*, 103, 701–708. 10.1016/j.ijbiomac.2017.05.054 [PubMed: 28522397]
- Palo M, Holländer J, Suominen J, Yliruusi J, & Sandler N (2017). 3D printed drug delivery devices: perspectives and technical challenges. *Expert Review of Medical Devices*, 14(9), 685–696. 10.1080/17434440.2017.1363647 [PubMed: 28774216]
- Peka M (2015, January 28). Hydrogels with micellar hydrophobic (nano)domains. *Frontiers in Materials*. Frontiers Media S.A. 10.3389/fmats.2014.00035
- Poudel AJ, He F, Huang L, Xiao L, & Yang G (2018). Supramolecular hydrogels based on poly (ethylene glycol)-poly (lactic acid) block copolymer micelles and α -cyclodextrin for potential injectable drug delivery system. *Carbohydrate Polymers*, 194, 69–79. 10.1016/j.carbpol.2018.04.035 [PubMed: 29801860]
- Pour Khalili N, Moradi R, Kavehpour P, & Islamzade F (2020). Boron nitride nanotube clusters and their hybrid nanofibers with polycaprolactone: Thermo-pH sensitive drug delivery functional materials. *European Polymer Journal*, 127, 109585. 10.1016/j.eurpolymj.2020.109585
- Qu J, Zhao X, Liang Y, Zhang T, Ma PX, & Guo B (2018). Antibacterial adhesive injectable hydrogels with rapid self-healing, extensibility and compressibility as wound dressing for joints skin wound healing. 10.1016/j.biomaterials.2018.08.044
- Qu Y, Tang J, Liu L, Song L, Chen S, & Gao Y (2019). α -Tocopherol liposome loaded chitosan hydrogel to suppress oxidative stress injury in cardiomyocytes. *International Journal of Biological Macromolecules*, 125, 1192–1202. 10.1016/j.ijbiomac.2018.09.092 [PubMed: 30227207]
- Sarkar N, & Bose S (2019). Liposome-Encapsulated Curcumin-Loaded 3D Printed Scaffold for Bone Tissue Engineering. *ACS Applied Materials & Interfaces*, 11(19), 17184–17192. 10.1021/acsami.9b01218 [PubMed: 30924639]
- Schwabe K, Ewe A, Kohn C, Loth T, Aigner A, Hacker MC, & Schulz-Siegmund M (2017). Sustained delivery of siRNA poly- and lipopolyplexes from porous macromer-crosslinked gelatin gels. *International Journal of Pharmaceutics*, 526(1–2), 178–187. 10.1016/j.ijpharm.2017.04.065 [PubMed: 28456652]
- Shahrezaee M, Salehi M, Keshtkari S, Oryan A, Kamali A, & Shekarchi B (2018). In vitro and in vivo investigation of PLA/PCL scaffold coated with metformin-loaded gelatin nanocarriers in regeneration of critical-sized bone defects. *Nanomedicine: Nanotechnology, Biology and Medicine*, 14(7), 2061–2073. 10.1016/j.nano.2018.06.007 [PubMed: 29964218]
- Smits EAW, Soetekouw JA, Pieters EHE, Smits CJP, de Wijs-Rot N, & Vromans H (2019). The availability of drug by liposomal drug delivery. *Investigational New Drugs*, 37(5), 890–901. 10.1007/s10637-018-0708-4 [PubMed: 30547315]
- Song T-H, Jang J, Choi Y-J, Shim J-H, & Cho D-W (2015). 3D-Printed Drug/Cell Carrier Enabling Effective Release of Cyclosporin A for Xenogeneic Cell-Based Therapy. *Cell Transplantation*, 24, 2513–2525. 10.3727/096368915X686779 [PubMed: 25608278]
- Thapa RK, Kiick KL, & Sullivan MO (2020). Encapsulation of collagen mimetic peptide-tethered vancomycin liposomes in collagen-based scaffolds for infection control in wounds. *Acta Biomaterialia*, 103, 115–128. 10.1016/j.actbio.2019.12.014 [PubMed: 31843720]
- Thilan De Silva R, Dissanayake RK, M G Prasanga Gayanath Mantilaka MM, Sanjeewa Lakmal Wijesinghe WP, Shalinda Kaleel S, Nisansala Premachandra T, ... Lanka S (2018). Drug-Loaded Halloysite Nanotube-Reinforced Electrospun Alginate-Based Nanofibrous Scaffolds with Sustained Antimicrobial Protection. 10.1021/acsami.8b11013
- Trenfield SJ, Awad A, Goyanes A, Gaisford S, & Basit AW (2018). 3D Printing Pharmaceuticals: Drug Development to Frontline Care. *Trends in Pharmacological Sciences*, 39(5), 440–451. 10.1016/j.tips.2018.02.006 [PubMed: 29534837]
- Uziel A, Shpigel T, Goldin N, & Lewitus DY (2019). Three-dimensional printing for drug delivery devices: a state-of-the-art survey. *Journal of 3D Printing in Medicine*, 3(2), 95–109. 10.2217/3dp-2018-0023
- Wang H, Wu G, Zhang J, Zhou K, Yin B, Su X, ... Wu Z (2016). Osteogenic effect of controlled released rhBMP-2 in 3D printed porous hydroxyapatite scaffold. *Colloids and Surfaces B: Biointerfaces*, 141, 491–498. 10.1016/j.colsurfb.2016.02.007 [PubMed: 26896655]

- Zhang Y, Zhang J, Chen M, Gong H, Thamphiwatana S, Eckmann L, ... Zhang L (2016). A Bioadhesive Nanoparticle–Hydrogel Hybrid System for Localized Antimicrobial Drug Delivery. *ACS Applied Materials & Interfaces*, 8(12), 8078–8087. 10.1021/acsami.6b04858
- Zhang Z, He Z, Liang R, Ma Y, Huang W, Jiang R, ... Li X (2016). Fabrication of a Micellar Supramolecular Hydrogel for Ocular Drug Delivery. *Biomacromolecules*, 17(3), 798–807. 10.1021/acs.biomac.5b01526 [PubMed: 26830342]
- Zhang ZZ, Zhang HZ, & Zhang ZY (2019). 3D printed poly(ϵ -caprolactone) scaffolds function with simvastatin-loaded poly(lactic-co-glycolic acid) microspheres to repair load-bearing segmental bone defects. *Experimental and Therapeutic Medicine*, 17(1), 79–90. 10.3892/etm.2018.6947 [PubMed: 30651767]
- Zhou Z, Yao Q, Li L, Zhang X, Wei B, Yuan L, & Wang L (2018). Antimicrobial Activity of 3D-Printed Poly(ϵ -Caprolactone) (PCL) Composite Scaffolds Presenting Vancomycin-Loaded Polylactic Acid-Glycolic Acid (PLGA) Microspheres. *Medical Science Monitor*, 24, 6934–6945. 10.12659/MSM.911770 [PubMed: 30269152]
- Zhu W, Li Y, Liu L, Chen Y, & Xi F (2012). Supramolecular hydrogels as a universal scaffold for stepwise delivering Dox and Dox/cisplatin loaded block copolymer micelles. *International Journal of Pharmaceutics*, 437, 11–19. 10.1016/j.ijpharm.2012.08.007 [PubMed: 22902390]

Further Reading

- Pitorre M, Gondé H, Haury C, Messous M, Poilane J, Boudaud D, ... Bastiat G (2017). Recent advances in nanocarrier-loaded gels: Which drug delivery technologies against which diseases? *Journal of Controlled Release*, 266(May), 140–155. 10.1016/j.jconrel.2017.09.031 [PubMed: 28951319]
- Dong Y, Wang S, Ke Y, Ding L, Zeng X, Magdassi S, & Long Y (2020). 4D Printed Hydrogels: Fabrication, Materials, and Applications. *Advanced Materials Technologies*, 5(6), 2000034. 10.1002/admt.202000034
- Ma K, Zhao T, Yang L, Wang P, Jin J, Teng H, ... Wang X (2020). Application of robotic-assisted in situ 3D printing in cartilage regeneration with HAMA hydrogel: An in vivo study. *Journal of Advanced Research*, 23, 123–132. 10.1016/j.jare.2020.01.010 [PubMed: 32099674]

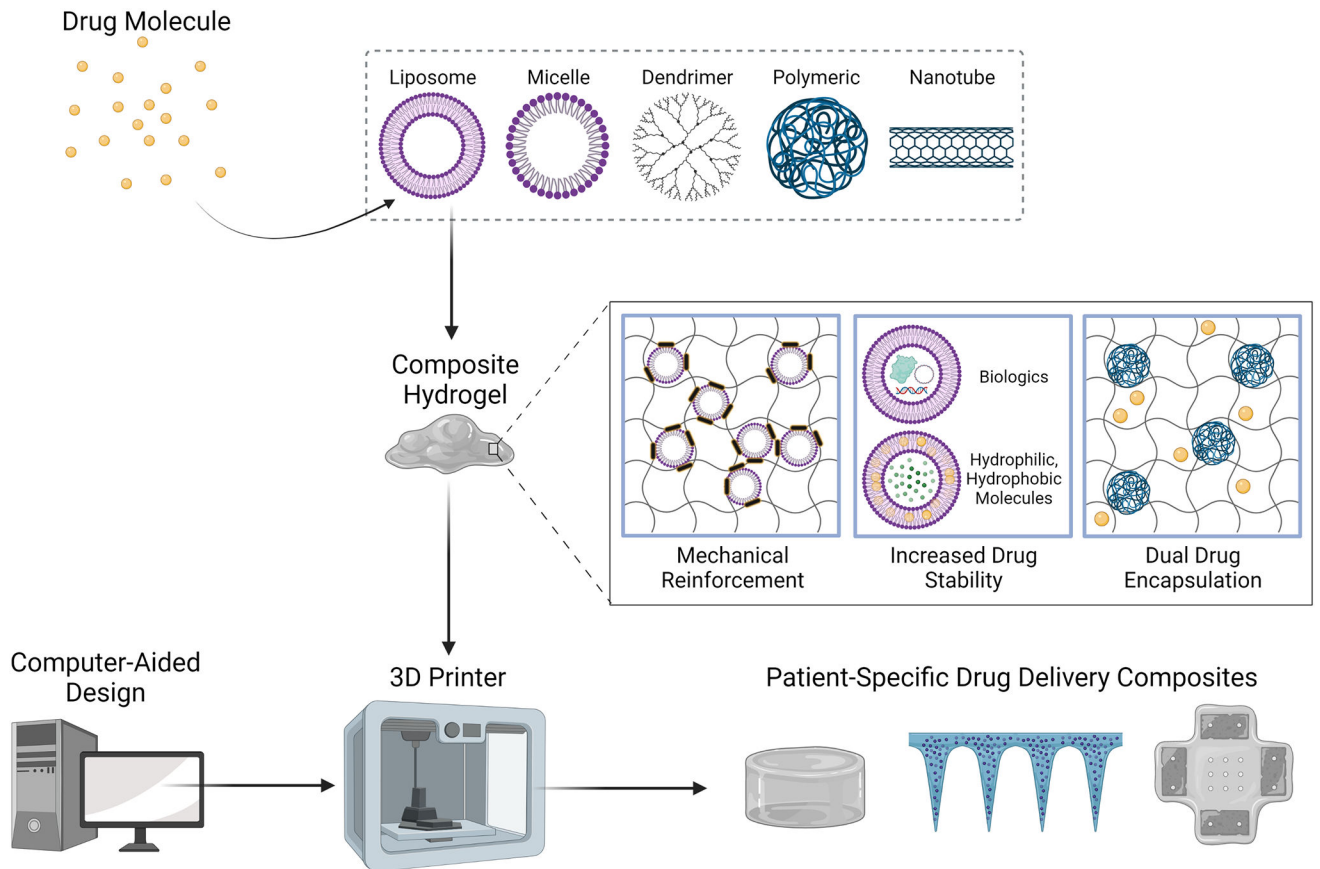


Figure 1. Nanocarrier-hydrogel composite materials can be formulated into a bioink from which customized drug delivery devices are generated via 3D printing.

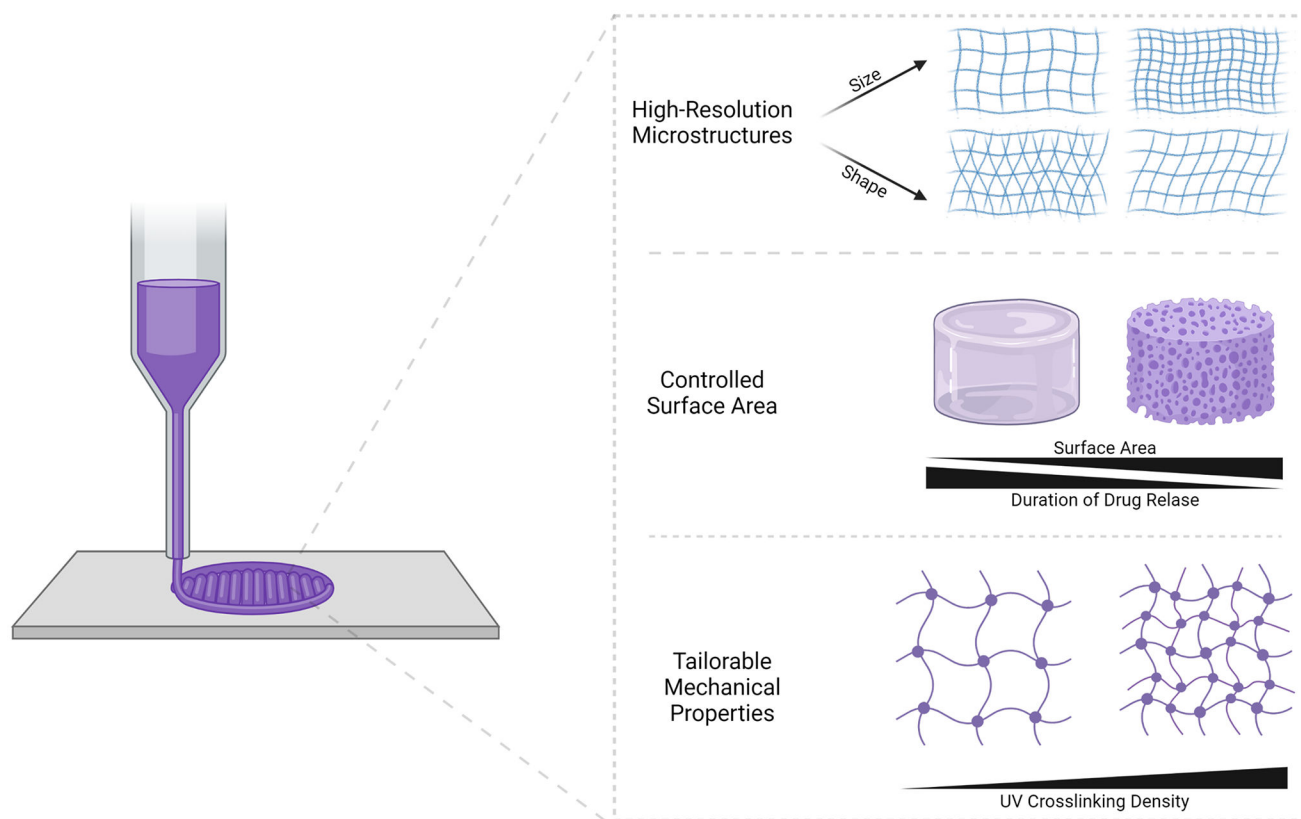


Figure 2. 3D printing offers control over the micro- and macrostructure and mechanical properties of the composite material, which can tailor drug release based on patient needs.

Table 1

Liposomal Hydrogels for Drug Delivery

Hydrogel Composition	Liposome Composition	Drug	Disease	Release	Release Profile	Method of Administration	Ref.
Collagen	N/A	Paclitaxel	Spinal cord injury repair	Hierarchical nano/microstructure provides sustained release of liposomes with the scaffold acting as a second barrier for release	Cumulative release of pristine drug 34% higher than release from liposomal scaffold at 24 hours	Scaffold implantation	(X. Li et al., 2018)
Collagen	DPPC, cholesterol, DSPE-PEG-Mal	Vanomycin	Infection	Liposome retention in the hydrogel enables sustained release which is primarily driven by drug diffusion through the liposome	Cumulative release extended 36 hours using CMP-tethered liposomal scaffold compared to pure drug-loaded scaffold	Topical	(Thapa et al., 2020)
Polyurethane	Lecithin, cholesterol, tocopherol	Paclitaxel	Breast cancer	Burst release is minimized by release of liposomes due to scaffold degradation, then drug release from liposome	Cumulative release from liposomal scaffold plateaus 144 hours longer than release from scaffolds containing Taxol	N/A	(Yin et al., 2020)
Polyethylene glycol	Lecithin, cholesterol, octadecylamine	BMP-2 peptide	Bone defects	Adhesive liposomes diffuse through the hydrogel to damaged tissue, where they attach and enable prolonged drug release	Adhesive liposomal scaffolds exhibit similar release profiles to normal liposomal scaffolds	Scaffold implantation	(L. Liu et al., 2019)
Chitosan, Eudragit RSPO, and polyvinyl alcohol	DSPC, cholesterol, DSPE	Galantamine	Alzheimer's	Drug release rate determined by the mechanical and physicochemical properties of the gel, which govern diffusional pathways	Cumulative release from non-crosslinked scaffolds up to 40% higher than release from crosslinked scaffolds at 50 days	Scaffold implantation	(Mufamadi et al., 2019)
Chitosan	Lecithin, cholesterol, sodium deoxycholate	alpha-tocopherol	Myocardial infarction	Liposome encapsulated drugs within the hydrogel exhibit sustained release with limited burst	Cumulative release from suspension-loaded scaffolds 16.6% higher than release from liposomal scaffolds at 140 hours	Subcutaneous injection	(Y. Qu et al., 2019)
N/A	PC-C32-PC, Me2PE-C32-Me2PE	Methylene Blue	Bacterial and fungal infection	Drug diffusion is limited by hydrophobic interactions or hydrophobic bonds formed with the bolalipid matrix	Drug release from the bolalipid scaffolds was 46% lower than that of a polymeric hydrogel after 8 hours	N/A	(Goergen et al., 2019)
N/A	PECE, EPC, cholesterol	Madecassoside	Wound healing	Drug diffuses through the bilayer membrane of the liposomes, which are immobilized due to PECE, thus sustaining release	Drug release from the PECE liposome hydrogel was 38% lower than that of a PECE hydrogel after 12 hours	Topical	(Meifeng Liu et al., 2020)
N/A	Phosphatidylcholine, cholesterol, thiolated chitosan	Curcumin	Breast cancer	Pore size controls drug release; higher concentrations of liposomes forming the hydrogel form hydrogels with smaller pores, limiting drug release	Drug release reached only 40% after 70 hours for hydrogels containing the highest concentration of liposomes	Injection	(R. Li et al., 2020)
Collagen®	DPPC	Anti-luciferase siRNA	N/A	Hydrogel properties (i.e. crosslinking density, pore size) governs lipopolyplex release	Cumulative release of lipopolyplexes from cGEL5 was	N/A	(Schwabe et al., 2017)

Hydrogel Composition	Liposome Composition	Drug	Disease	Release	Release Profile	Method of Administration	Ref.
Hydroxyethyl Cellulose	DOTAP, DOPE, cholesterol, DSPE-PEG	siRNA	Genital diseases	Hydrogel viscosity and concentration can be modified to sustain lipoplex release	equivalent to that of naked siRNA, but without burst release	Vaginal	(Furst et al., 2016)
pHEMA	StemFect™, Lipofectamine™	GFP-mRNA	Immunotherapy or vaccine applications	Lipoplex immobilization in the scaffold slows release and enhances transfection efficiency	Cumulative release of mRNA from lipoplex scaffolds is 3 times lower than systemic mRNA injection	Implantation	(R. Chen et al., 2018)
Chitosan, alginate	StemFect™	Ovalbumin-mRNA	Immunotherapy or vaccine applications	mRNA is released from the lipoplex scaffold as the hydrogel degrades with limited burst release	Release of lipoplexes reached 30% over 2 weeks, compared to 80% mRNA release from gels after 3 days	Subcutaneous Injection	(J. Yan et al., 2019)

Table 2

Micelle Hydrogels for Drug Delivery

Hydrogel Composition	Micelle Composition	Drug	Disease	Release	Release Profile	Method of Administration	Ref.
α -cyclodextrin	poly(ethylene glycol)- <i>b</i> -polycaprolactone, poly(ethylene glycol)- <i>b</i> -polyacrylic acid	Doxorubicin, cisplatin	Cancer	Micelles are released from the hydrogel with degradation, then drugs encapsulated in the micelles are released via diffusion	Cumulative release of DOX is reduced from 100% to 28% at 168 hours via cyclodextrin/micellar hydrogel	Injection	(Poudeh et al., 2018)
α -cyclodextrin	methoxy poly(ethylene glycol) block polymer	Diclofenac	Eye disease	Shear from blinking degrades the hydrogel and micellar drugs escape	Cumulative release of drug in solution is 95% at 12 hours, is extended to at least 91% at 216 hours using micellar hydrogel	Topical	(Z. Zhang et al., 2016)
N/A	methacrylated inulin/vitamin E	Beclomethasone dipropionate	Crohn's disease	Drug release is mainly dependent on the swelling behavior of the gels, which is impacted by UV crosslinking time	Cumulative release reaches 60% at 120 hours using nanogrids	N/A	(Mandracchia et al., 2018)
N/A	alginate- <i>g</i> -poly(N-isopropylacrylamide)	Doxorubicin	Cancer	As the hydrogel undergoes dissolution, micelles are released, and the drug diffused to the target in a sustained manner	Release of DOX is sustained up to 500 hours <i>in vitro</i>	Injection	(Min Liu et al., 2017)
Carboxymethyl chitosan	poly(ethylene oxide)/poly(propylene oxide)/poly(ethylene oxide)	Glutaraldehyde	Eye disease	Hydrogel properties are governed by pH and temperature, resulting in different release profiles because of differences in swelling and porosity	Cumulative release of drug solution reached 100% at 72 hours, is reduced to 80% at 72 hours with micellar gel	Topical	(S. Yu et al., 2017)
Quaternized chitosan	poly(ethylene oxide)- <i>b</i> -poly(propylene oxide)- <i>b</i> -poly(ethylene oxide)	Curcumin	Infection	The hydrogel matrix and crosslinking point Schiff base are pH sensitive, enabling drug release when in contact with the acidic environment of wounds	Release of Curcumin is sustained up to 300 hours <i>in vitro</i> depending on pH	Injection	(J. Qu et al., 2018)
Chitosan/oxidized dextran	poly(ethylene oxide)/poly(propylene oxide)/poly(ethylene oxide)	Curcumin, 5-fluoracil	Cancer	The hydrogel is redox and pH sensitive, which stimulates hydrogel degradation and drug release in the cancerous microenvironment	Release is sustained up to 9 days <i>in vitro</i> depending on the strength of the reductive environment	Injection	(Gao et al., 2016)
Chitosan	sulfobetaine/4-vinylphenylboronic acid / dialdehyde starch	Insulin, nattokinase	Diabetes	Micelles are responsive to glucose, which triggers insulin release	Release is sustained up to 72 hours <i>in vitro</i> depending on glucose levels	Injection	(Wen et al., 2019)

Table 3

Dendrimer Hydrogels for Drug Delivery

Hydrogel Composition	Dendrimer Composition	Drug	Disease	Release	Release Profile	Method of Administration	Ref.
Polyethylene glycol diacrylate	Polyamidoamine	Camptothecin	Cancer	Dendrimers are released slowly with microgel degradation, which is pH dependent, then camptothecin is released via diffusion from the dendrimer core	Cumulative release of free CPT reaches 100% at 24 hours, is reduced to 20% at 120 hours via dendrimer hydrogel encapsulation	Intravenous injection	(J. Wang et al., 2018)
Polyethylene glycol diacrylate	Polyamidoamine	Brimonidine tartrate	Glaucoma	Brimonidine free base and salt forms are released in burst from the loosely-crosslinked gel network, and brimonidine encapsulated in the dendrimer core is released slowly over time	Cumulative release of free BPT reaches 100% at 24 hours, is reduced to 100% at 48 hours via dendrimer hydrogel encapsulation	Topical	(J. Wang, Williamson, et al., 2017)
Polyethylene glycol bisazide	Polyamidoamine	5-fluorouracil	Cancer	5-fluorouracil in the loose hydrogel network is released in burst, whereas the 5-fluorouracil trapped within the dendrimer is released slowly over time	Cumulative release of free 5FU reaches 100% at 6 hours, is reduced to ~75% at 12 hours via dendrimer hydrogel encapsulation	Intratumoral injection	(L. Xu et al., 2017)
Polyethylene glycol diacrylate	Polyamidoamine	5-fluorouracil	Cancer	5-fluorouracil in the loose hydrogel network is released in burst, whereas the 5-fluorouracil trapped within the dendrimer is released slowly over time	Cumulative release of free 5FU reaches 70% in 30 minutes, is reduced to 60% at 1 hour (with a 6 hour plateau at 80%) via dendrimer hydrogel encapsulation	Intratumoral injection	(J. Wang, He, et al., 2017)
Polyethylene glycol diacrylate	Polyamidoamine	Camptothecin	Cancer	Self-cleaving of camptothecin from the dendrimer occurs via ammoniolysis, followed by diffusion through the hydrogel	Cumulative release of free CPT reaches 100% at 24 hours, is slowed to 100% at 144 hours via dendrimer hydrogel encapsulation	Intratumoral injection	(J. Wang et al., 2019)

Table 4

Polymeric Nanocarrier Hydrogels for Drug Delivery

Hydrogel Composition	Nanocarrier Composition	Drug	Disease	Release	Release Profile	Method of Administration	Ref.
GelMA, chitosan	Chitosan	BSA-bFGF	Promotion of angiogenesis	Biodegradation and crosslinking degree of the hydrogel enable sustained release of drug	Cumulative release reaches 90% and is sustained for 14 days <i>in vitro</i>	N/A	(Azizian et al., 2018)
Chitosan, gelatin	Chitosan	BSA-bFGF	Delivery to cells for enhanced growth	Sustained release enhanced by Chitosan-gelatin scaffold which acts as a second barrier to drug release	Cumulative release reaches 100% at 50 hours <i>in vitro</i>	N/A	(Modaresifar et al., 2017)
Chitosan	Chitosan	BMP-2 plasmid DNA	Bone defects	Thermoresponsivity and degradation drive drug release	N/A	Implantation	(H. Li et al., 2017)
Acrylamide, poly(ethylene glycol) dimethacrylate, polyvinyl alcohol	Poly(lactic-co-glycolic acid)	Ciprofloxacin	Infection	Hydrogel degradation and diffusion of drug from nanoparticles enable controlled drug release	Cumulative Cipro release from blank gels reaches ~94% in 12 hours, is slowed to 88.2% in 72 hours with nanoparticle gels	Topical	(Y. Zhang et al., 2016)
Poly lactic acid, polycaprolactone	Gelatin	Metformin	Bone defects	Sustained release enhanced by PLA/PCL scaffold which acts as a second barrier to drug release	Cumulative MET release from nanocarrier scaffolds is decreased over 14 days compared to release from nanocarriers alone	Implantation	(Shahrezaee et al., 2018)
Cellulose acetate/poly(lactic acid)	Gelatin	Citalopram	Nerve defects	Nanocarrier-coated scaffolds exhibit increased biodegradability, which facilitates drug release	N/A	Implantation	(Naseri-Nosar et al., 2017)

Table 5

Nanotube Hydrogels for Drug Delivery

Hydrogel Composition	Nanotube Composition	Drug	Disease	Release	Release Profile	Method of Administration	Ref.
Gelatin	Halloysite	Ibuprofen	Infection, pain	Nanotube incorporation reinforces hydrogel mechanically and limits diffusion of drug compared to drug-loaded gelatin	Cumulative release of IBU from Gelatin reached 100% in 10 hours, is slowed to 100% in ~100 hours with nanotube composite scaffold	Implantation	(Ji et al., 2017)
Alginate	Halloysite	Cephalixin	Antiseptic	Crosslinking of alginate nanofibers limits drug diffusion through the matrix, sustaining drug release compared to release from nanotubes alone	Cumulative release of CEF from HNTs alone reached 95% in 24 hours, is slowed to 89% in 7 days with nanotube composite scaffold	Implantation	(Thilan De Silva et al., 2018)
Poly(L-lactide)	Halloysite	Polymyxin B Sulfate	Infection	Nanotubes impact polymer degradation, enabling control over release from hydrogel-encapsulated drug and nanotube-encapsulated drug	Cumulative release of PMB from HNTs alone reached 100% in 20 days, is slowed to 40% in 35 days with nanotube composite scaffold	Implantation	(X. Zhang et al., 2015)
Polycaprolactone	Boron nitride	Doxorubicin	Cancer	Drug release can be tuned by pH and temperature due to nanotube cluster formation and degradation, respectively	BNNT composite scaffolds provide slower, more stable release of DOX compared to BNNT delivery alone; the release kinetics can be controlled with pH and temperature	N/A	(Pour Khalili et al., 2020)
Chitosan	Halloysite	4-aminopyridine	Nerve repair	Crosslinking of chitosan-nanotube composites limits drug diffusion through the matrix, sustaining drug release	Cumulative release of 4AP from Chitosan reached 98% in 30 minutes, is slowed to 30% in 7 days with crosslinked nanotube composite scaffold	Implantation	(Manoukian, Arul, Rudraiah, Kalazic, & Kumbhar, 2019)

Table 6

3D-Printed Nanocomposite Hydrogels for Drug Delivery

Hydrogel Composition	Nanocarrier Type	3D Printing Method	Drug	Disease	Notes	Ref.
Pluronic F127	Micelle	Direct-write	N/A	N/A	Salt concentration and pH control micelle stability, printing resolution, and swelling	(Berry et al., 2019)
Poloxamer 407	Micelle	Fused deposition	Paclitaxel	Ovarian cancer	Sol-gels exhibit biphasic drug release due to rapid erosion, whereas 3D-printed discs exhibit single-phase release	(Cho et al., 2019)
Poly(lactic acid)	Nanotube	Syringe extrusion	Gentamicin	Infection		(Weisman et al., 2017)
Polycaprolactone	Liposome	Syringe extrusion	Ruthenium	Osteosarcoma	3D printing enables controlled porosity for biomimetic bone structure	(Ye et al., 2019)
Calcium phosphate	Liposome	Binder jet printing	Curcumin	Osteosarcoma	3D printing enables controlled porosity for biomimetic bone structure	(Sarkar & Bose, 2019)
Fish gelatin methacryloyl	Liposome	Semi-solid extrusion	Doxorubicin	Various cancers	Torus, cylinder, and gridline structures exhibit differences in drug release due to crosslinking density and surface area	(J. Liu et al., 2020)
Polycaprolactone	Liposome	Syringe extrusion	Aspirin	Bone defects		(Y. Li et al., 2019)
Polycaprolactone	Liposome	N/A	Aspirin	Bone defects		(Y. Li et al., 2020)
Gelatin, alginate, tricalcium phosphate	Polymeric Carrier	Syringe extrusion	VEGF	Bone defects	3D printing enables controlled porosity for biomimetic bone structure	(Fahimipour et al., 2017)
Polycaprolactone	Polymeric Carrier	Fused deposition	Vancomycin	Bone infections	3D printing enables controlled porosity for biomimetic bone structure	(Zhou et al., 2018)
Polycaprolactone	Polymeric Carrier	Fused deposition	Simvastatin	Bone defects	3D printing enables controlled porosity for biomimetic bone structure	(Z. Z. Zhang et al., 2019)
Alginate	Polymeric Carrier	Solid freeform fabrication	Cyclosporin A	Immunosuppressive	Structural stability from 3D-printed scaffold helps device maintain structure up to 4 weeks <i>in vivo</i>	(Song et al., 2015)
Gelatin methacrylate	Polymeric Carrier	Digital light processing	RGFP966	Nerve regeneration		(X. Xu et al., 2019)
Hydroxyapatite	Polymeric Carrier	Extrusion deposition	rhBMP2	Bone defects	3D printing enables controlled porosity for biomimetic bone structure	(H. Wang et al., 2016)